

# UC Berkeley

## UC Berkeley Previously Published Works

### Title

Cr(110) texture induced by epitaxy on Al<sub>2</sub>O<sub>3</sub>(0001) substrates: Preferential grain growth in the [001] direction

### Permalink

<https://escholarship.org/uc/item/5bz7q1p7>

### Journal

Applied Physics Letters, 102(14)

### ISSN

0003-6951

### Authors

Boekelheide, Z  
Hellman, F

### Publication Date

2013-04-08

### DOI

10.1063/1.4801083

Peer reviewed

## Cr(110) texture induced by epitaxy on $\text{Al}_2\text{O}_3(0001)$ substrates: Preferential grain growth in the $\langle 001 \rangle$ direction

Z. Boekelheide<sup>1,2,3,a)</sup> and F. Hellman<sup>2,3</sup>

<sup>1</sup>Material Measurement Laboratory, National Institute of Standards and Technology, Gaithersburg, Maryland 20899, USA

<sup>2</sup>Department of Physics, University of California, Berkeley, Berkeley, California 94720, USA

<sup>3</sup>Materials Sciences Division, Lawrence Berkeley National Laboratory, Berkeley, California 94720, USA

(Received 27 September 2012; accepted 26 March 2013; published online 8 April 2013)

Chromium exhibits (110) textured growth on  $\text{Al}_2\text{O}_3(0001)$  substrates induced by epitaxy. Epitaxy occurs in nine distinct orientations, leading to a polycrystalline film of grains with (110) out-of-plane orientation but different in-plane orientations. For e-beam evaporated films, scanning electron microscopy shows acicular Cr grains elongated in the  $\langle 001 \rangle$  direction. Grain boundaries occur along  $(1\bar{1}0)$  and  $(\bar{1}10)$  planes, which is explained by the low surface energy of  $\{110\}$  planes in the bcc structure. The direction of the long axes of the grains relative to the substrate is defined by the underlying hexagonal symmetry of the substrate, leading to a unique tri-directional microstructure. © 2013 AIP Publishing LLC. [<http://dx.doi.org/10.1063/1.4801083>]

Chromium is an important material in engineering of thin film heterostructures. Cr bonds well to oxide substrates because of its fairly high oxygen affinity, and the chromium oxide at the interface is self-limiting.<sup>1</sup> In addition, Cr is inexpensive, making it a popular choice for an adhesion layer. Cr is also antiferromagnetic and is used in magnetic heterostructures as, for example, the nonmagnetic layer in Fe/Cr giant magnetoresistive multilayers or for the antiferromagnetic pinning layer in exchange biased heterostructures.<sup>2,3</sup> Thus, the behavior of Cr films on a variety of substrates is of interest.

Chromium crystallizes in the body centered cubic structure, and for epitaxial growth, the cubic MgO substrate is commonly chosen.<sup>4</sup> However, sapphire is another possible choice of substrate. Epitaxial growth of Cr(110) on  $\text{Al}_2\text{O}_3(0001)$  (C-plane sapphire) has been studied previously, experimentally by transmission electron microscopy<sup>5</sup> and theoretically.<sup>6</sup> Because the (0001) surface of  $\text{Al}_2\text{O}_3$  has hexagonal symmetry while the Cr(110) surface has rectangular symmetry, multiple orientations are possible in the plane. The result is a polycrystalline Cr film with strong out-of-plane texture due to epitaxy of the individual grains on the substrate.

This paper discusses the epitaxial growth of e-beam evaporated Cr(110) on  $\text{Al}_2\text{O}_3(0001)$ , with characterization by reflection high energy electron diffraction (RHEED), x-ray diffraction (XRD), and scanning electron microscopy (SEM). We find that for e-beam evaporated films, the epitaxial grains have an elongated (acicular) shape. The long axes of these grains point along three major directions defined by the substrate, resulting in a tri-directional microstructure. Analysis shows that the grains are elongated along the  $\langle 001 \rangle$  direction, with grain boundaries occurring along  $(1\bar{1}0)$  and  $(\bar{1}10)$  planes, due to the low surface energy of  $\{110\}$  planes in the bcc structure.

Cr films were grown by e-beam evaporation at a rate of 0.03 nm/s and a base pressure below  $7 \times 10^{-6}$  Pa ( $5 \times 10^{-8}$

Torr) onto  $\text{Al}_2\text{O}_3(0001)$  (C-plane sapphire) substrates held at 300 °C during growth. Cr films grown under these conditions show less than  $3 \pm 1$  at. % oxygen incorporated, confirmed by oxygen-resonant Rutherford backscattering spectroscopy (RBS) and electron dispersive spectroscopy (EDS), with no other contaminants detected.

Film growth was monitored *in situ* by RHEED. After the films were removed from the sample chamber, they were characterized by (XRD) with a 4-circle diffractometer using Cu  $K\alpha_1$  radiation. Film microstructure was studied by SEM. Film thickness was measured with an Alpha-Step IQ profilometer at several points and averaged. All uncertainties reported here represent one standard deviation.

RHEED patterns for a  $(88 \pm 6)$  nm thick Cr/ $\text{Al}_2\text{O}_3(0001)$  film are shown in Figure 1. Fig. 1(a) shows the pattern for the bare  $\text{Al}_2\text{O}_3(0001)$  substrate before film growth. Fig. 1(b) shows the pattern of the Cr film after deposition was completed. The spotted pattern indicates epitaxy with three-dimensional growth.<sup>1</sup> The pattern seen in Fig. 1(b) is a superposition of a square and a triangular lattice of diffraction spots, shown overlaid on the RHEED pattern as blue and red spots in Fig. 1(c). The square pattern is associated with Cr(110) out-of-plane oriented crystallites with the electron beam oriented along a  $\langle 001 \rangle$  direction in the plane (Fig. 1(d)). The triangular pattern is associated with Cr(110) out-of-plane oriented crystallites with the electron beam oriented along  $\langle 1\bar{1}\bar{1} \rangle$  or  $\langle \bar{1}1\bar{1} \rangle$  directions in the plane (Fig. 1(e)). This superposition of patterns suggests a highly textured Cr(110) film with grains with multiple in-plane orientations.

Figure 2 shows the XRD characterization of a  $(153 \pm 3)$  nm thick Cr/ $\text{Al}_2\text{O}_3(0001)$  film. Part (a) shows a  $\theta - 2\theta$  scan showing sharp Cr (110) and (220) peaks, with no peaks from other Cr orientations. This suggests strong Cr(110) texture out of plane. Azimuthal ( $\phi$ ) scans were performed to probe the epitaxy. Figure 2(b) shows a  $\phi$  scan of the off-axis  $\text{Al}_2\text{O}_3\{1\bar{1}02\}$  (R-plane) peaks, measured at 52.583° from normal, showing the three-fold symmetry of the  $\text{Al}_2\text{O}_3$  single-crystal substrate. Figure 2(c) shows a  $\phi$  scan of the Cr  $\{100\}$  peaks, measured at 45° from normal, which show six-fold symmetry. The Cr

<sup>a)</sup>zoe.boekelheide@nist.gov. Address as of 1 July 2013: Physics Department, Lafayette College, Easton, Pennsylvania 18042, USA; email: boekelhz@lafayette.edu

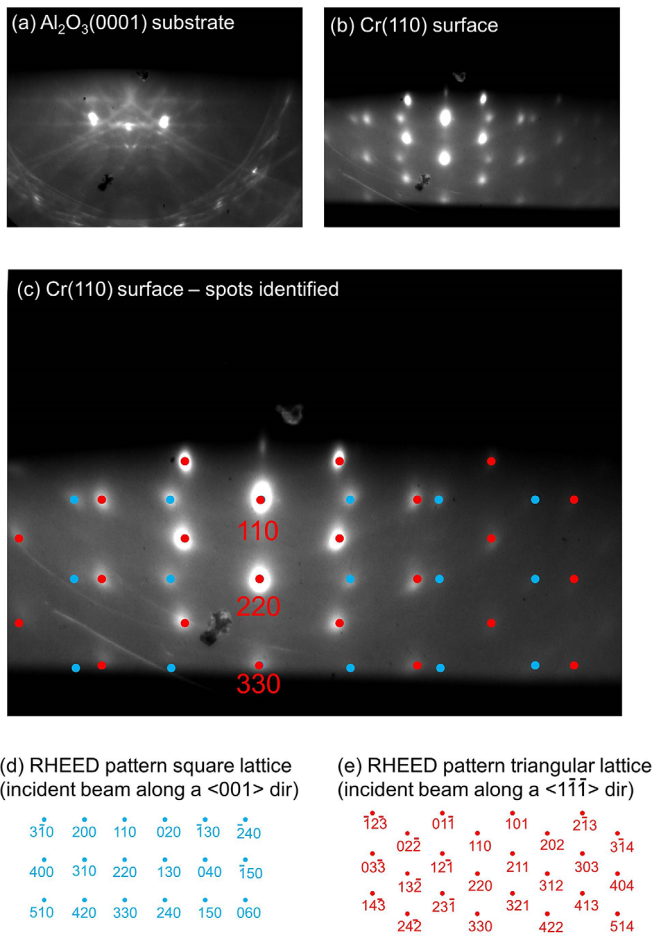


FIG. 1. RHEED patterns for (a) bare  $\text{Al}_2\text{O}_3(0001)$  substrate and (b) Cr(110)/ $\text{Al}_2\text{O}_3(0001)$  film after deposition. Part (c) shows the RHEED pattern from (b) with a superposition of two indexed patterns overlaid in blue and red. The two diffraction patterns are (d) a square lattice diffraction pattern associated with the Cr(110) surface with the incident electron beam along a  $\langle 001 \rangle$  direction in the plane and (e) a triangular lattice diffraction pattern of the Cr(110) surface with the incident beam along a  $\langle 1\bar{1}\bar{1} \rangle$  or  $\langle \bar{1}11 \rangle$  direction in the plane. The 110 spots of the two patterns overlap.

{100} peaks are broad, with a full-width at half maximum (FWHM) of  $11.3^\circ \pm 0.1^\circ$  in  $\phi$ .

Cr(110)/ $\text{Al}_2\text{O}_3(0001)$  epitaxy occurs with two possible in-plane orientation relationships.<sup>5,6</sup> We call these Orientation Relationship I and II (OR-I and OR-II). OR-I is also called Pitsch-Schrader<sup>6</sup> or Nishiyama-Wasserman.<sup>5</sup> OR-II is also called Burgers<sup>6</sup> or Kurdjumov-Sachs.<sup>5</sup> The orientation relationships are as follows:<sup>6</sup>

$$\begin{aligned}
 \text{OR-I : } & \text{Cr}(110) \parallel \text{Al}_2\text{O}_3(0001)(\text{C-plane}) \\
 & \text{Cr}[001] \parallel \text{Al}_2\text{O}_3[10\bar{1}0](\text{M-direction}) \\
 & \text{Cr}[\bar{1}10] \parallel \text{Al}_2\text{O}_3[1\bar{2}10](\text{A-direction}) \\
 \text{OR-II : } & \text{Cr}(110) \parallel \text{Al}_2\text{O}_3(0001)(\text{C-plane}) \\
 & \text{Cr}[\bar{1}11] \parallel \text{Al}_2\text{O}_3[1\bar{1}00](\text{M-direction}) \\
 & \text{Cr}[\bar{1}\bar{1}\bar{2}] \parallel \text{Al}_2\text{O}_3[\bar{1}\bar{1}20](\text{A-direction}).
 \end{aligned} \tag{1}$$

These epitaxial relations are shown graphically in Figure 3. Because  $\text{Al}_2\text{O}_3$  has hexagonal symmetry while Cr has cubic symmetry, there are three different in-plane orientations which satisfy OR-I. OR-II is similar to OR-I but rotated  $5.26^\circ$  to the right or left of OR-I. Thus, six possible in-plane orientations exist which satisfy OR-II.

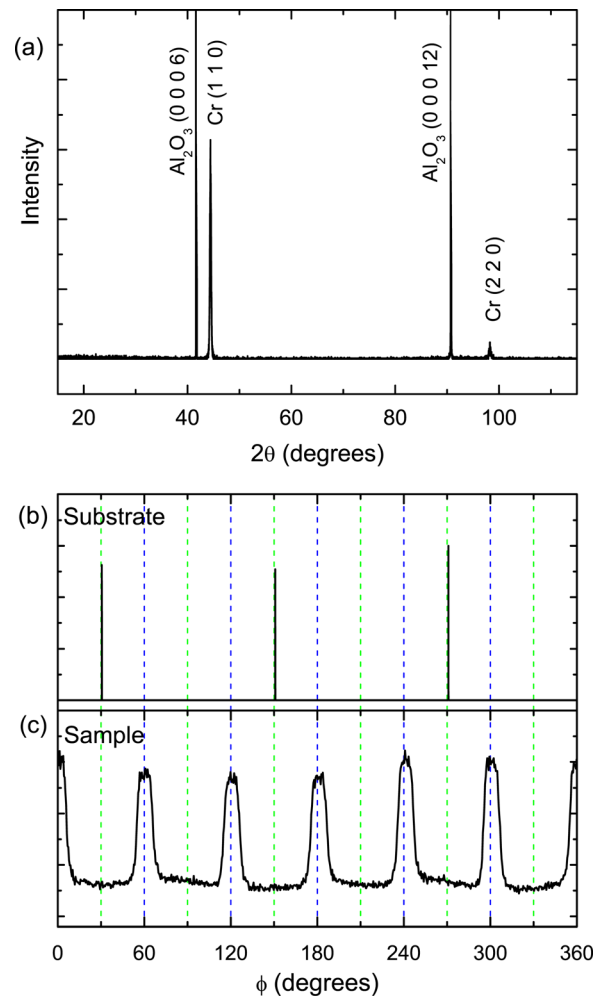


FIG. 2. (a)  $\theta - 2\theta$  scan showing only Cr (110) orientation out of plane. (b) and (c)  $\phi$  (azimuthal) scans of (b) the  $\text{Al}_2\text{O}_3$  substrate  $\{1\bar{1}02\}$  (R-plane) peaks measured at  $52.583^\circ$  from normal and (c) Cr sample  $\{100\}$  peaks measured at  $45^\circ$  from normal.

The azimuthal XRD scans in Fig. 2(c) are consistent with this set of nine OR-I and OR-II orientations in the Cr film. A (110) oriented single crystal of Cr would show only two peaks in such an azimuthal scan: (100) and (010), as shown in the stereographic projection in Fig. 4(d). The three

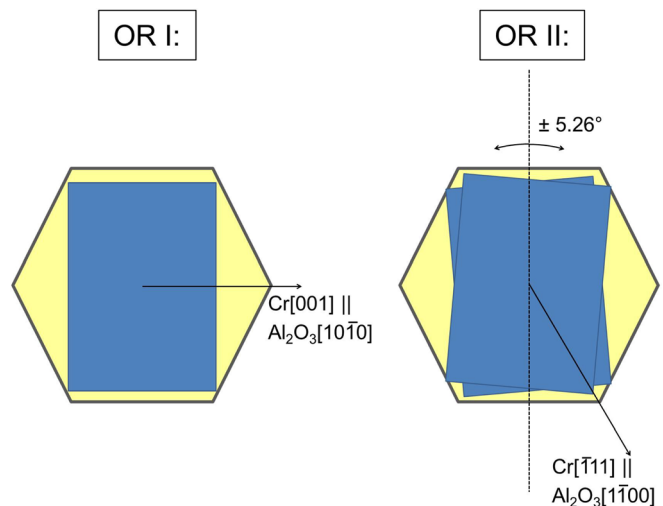


FIG. 3. Graphical representation of orientation relationships OR-I and OR-II.

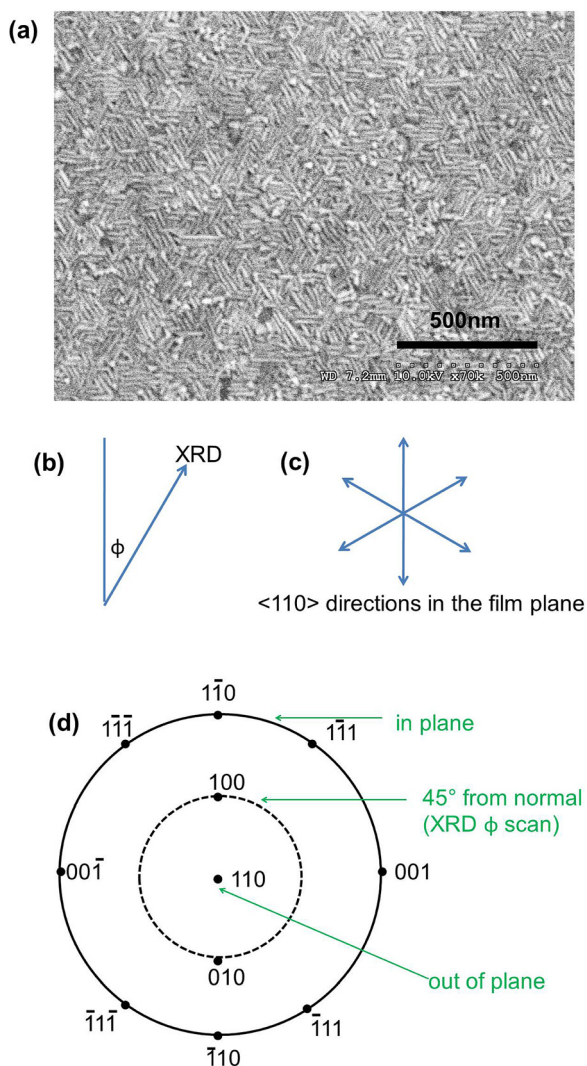


FIG. 4. (a) SEM image of Cr(110)/Al<sub>2</sub>O<sub>3</sub>(0001) film. (b) Definition of angle  $\phi$  referenced to Figure 2. (c) Cr  $\langle 110 \rangle$  directions in the film plane, inferred from XRD. (d) Stereographic projection of cubic Cr(110), adapted from Ref. 7. The central spot represents the normal direction, the dotted line represents points 45° from normal, and the solid line represents points 90° from normal (in the plane of a film).

orientations satisfying OR-I each contribute these two peaks, for a total of six peaks as seen in Fig. 2(c). The six orientations satisfying OR-II occur rotated at  $\pm 5.26^\circ$  from OR-I and lead to the broadening of the azimuthal peaks. The width of the peaks (FWHM =  $11.3^\circ$ ) is consistent with this model.

The superposition of diffraction patterns seen in RHEED (Fig. 1) is also consistent with these two orientation relationships. The patterns are associated with  $\langle 001 \rangle$ ,  $\langle 1\bar{1}\bar{1} \rangle$ , and  $\langle \bar{1}\bar{1}\bar{1} \rangle$  directions parallel to the beam in the film plane. These directions are coincident with the Al<sub>2</sub>O<sub>3</sub> M-direction under the OR-I and OR-II schemes, respectively.

An SEM image of the  $(153 \pm 3)$  nm film is shown in Figure 4(a). The image shows the polycrystalline nature of the film, with elongated, acicular grains. The grains are preferentially oriented with their long axes along three directions. The SEM image can be compared with the XRD data of the same sample in Fig. 2. The azimuthal angle  $\phi$  in the XRD measurement is defined relative to the SEM image as shown in Fig. 4(b).

The  $\{100\}$  peaks seen in Fig. 2(c), measured at 45° from normal, occur at  $\phi = 0^\circ, 60^\circ, 120^\circ, 180^\circ, 240^\circ,$  and  $300^\circ$ .

The stereographic projection shown in Fig. 4(d) shows that these angles correspond to  $\langle 110 \rangle$  directions in the plane. Thus, the  $\langle 110 \rangle$  directions are oriented in the film plane as shown in Fig. 4(c). The grains appear elongated along the directions  $\phi = 30^\circ, 90^\circ, 150^\circ, 210^\circ, 270^\circ,$  and  $330^\circ$ , which means that the grains are elongated along the  $\langle 100 \rangle$  directions, with grain boundaries occurring on the  $\{110\}$  planes. This is consistent with the  $\{110\}$  planes in the bcc structure having the lowest energy. A similar effect has been seen in Fe films grown on Au(111) surfaces.<sup>8</sup>

Grain formation in thin films is a complex balance of thermal energy, surface energy, and grain boundary energy. Acicular or elongated grains only occur for a subset of deposition conditions.<sup>9–12</sup> Thus, not all Cr(110)/Al<sub>2</sub>O<sub>3</sub>(0001) films will show this unique microstructure.

In addition to energy effects, momentum and shadowing effects can play a role in elongating and orienting grains.<sup>11,13</sup> Thus, it may be possible to use the epitaxy described here and a directional effect, such as sputtering from an angled source or ion-beam assisted deposition, to define acicular grains in a single direction. Such a development would be useful in applications, for example, as a template for patterned media for future hard disk data storage.

In conclusion, Cr grows epitaxially, in the (110) direction, on Al<sub>2</sub>O<sub>3</sub>(0001) (C-plane sapphire). There are multiple in-plane orientation relationships, creating a polycrystalline film where each grain is epitaxial with the substrate, but neighboring grains are oriented differently from each other in the plane. This results in an interesting microstructure where the long  $\langle 100 \rangle$  axes of the acicular grains point along three directions defined by the hexagonal nature of the substrate.

The authors thank Eduardo Saiz for assistance with the SEM, Hyeon-Jun Lee for assistance with the XRD, and Julie Karel for assistance with the e-beam evaporator. The experimental portion of this work was supported by the U.S. Department of Energy under Contract No. DE-AC02-05CH11231. Z. Boekelheide acknowledges the funding support of the NRC Research Associateship Program at NIST during the analysis portion of this work.

<sup>1</sup>D. L. Smith, *Thin-Film Deposition: Principles & Practice* (McGraw Hill, San Francisco, 1995).

<sup>2</sup>M. N. Baibich, J. M. Broto, A. Fert, F. N. V. Dau, F. Petroff, P. Etienne, G. Creuzet, A. Friederich, and J. Chazelas, *Phys. Rev. Lett.* **61**, 2472 (1988).

<sup>3</sup>J. S. Parker, L. Wang, K. A. Steiner, P. A. Crowell, and C. Leighton, *Phys. Rev. Lett.* **97**, 227206 (2006).

<sup>4</sup>E. E. Fullerton, M. J. Conover, J. E. Mattson, C. H. Sowers, and S. D. Bader, *Phys. Rev. B* **48**, 15755 (1993).

<sup>5</sup>S. Tsukimoto, F. Phillipp, and T. Wagner, *J. Eur. Ceram. Soc.* **23**, 2947 (2003).

<sup>6</sup>C. M. Montesa, N. Shibata, T. Tohei, K. Akiyama, Y. Kuromitsu, and Y. Ikuhara, *Mater. Sci. Eng. B* **173**, 234 (2010).

<sup>7</sup>B. Fulz and J. Howe, *Transmission Electron Microscopy and Diffractometry of Materials* (Springer, New York, 2002).

<sup>8</sup>M. Cahoreau and M. Gillet, *Surf. Sci.* **26**, 415 (1971).

<sup>9</sup>Z. Boekelheide, E. Helgren, and F. Hellman, *Phys. Rev. B* **76**, 224429 (2007).

<sup>10</sup>Z. Boekelheide, D. W. Cooke, E. Helgren, and F. Hellman, *Phys. Rev. B* **80**, 134426 (2009).

<sup>11</sup>Z. B. Zhao, S. M. Yalisove, Z. U. Rek, and J. C. Bilello, *J. Appl. Phys.* **92**, 7183 (2002).

<sup>12</sup>Z. B. Zhao, Z. U. Rek, S. M. Yalisove, and J. C. Bilello, *Thin Solid Films* **472**, 96 (2005).

<sup>13</sup>S. Iwatsubo and M. Naoe, *IEEE Trans. Magn.* **37**, 2298 (2001).